PROCEEDINGS OF SCIENCE

MAGIC observations of the putative PeVatron SNR G106.3+2.7 in the proximity of the Boomerang PWN

Takayuki Saito[a,*], **Tomohiko Oka**[b], **Marcel Strzys**[a] **and Hidetoshi Kubo**[a]
on behalf of the MAGIC collaboration

[a] *Institute of Cosmic Ray Research, Univ. Tokyo, Kashiwanoha 5-1-5, Kashiwa-shi, Chiba, Japan*
[b] *Kyoto University, Kitashirakawa Oiwakecho, Sakyo-ku Kyoto, Japan*
E-mail: tsaito@icrr.u-tokyo.ac.jp, oka.tomohiko.25n@st.kyoto-u.ac.jp, strzys@icrr.u-tokyo.ac.jp, kubo@icrr.u-tokyo.ac.jp

We observed one of the most promising PeVatron candidates, SNR G106.3+2.7 with the MAGIC telescope for 122 hours in total between May 2017 and August 2019. We detected extended γ-ray emission spatially coincident with the radio continuum, which exhibits a cometary shape with a head and a tail region. A significant γ-ray emission with energies above 6.0 TeV was detected only from the tail region, suggesting that the emissions above 10 TeV, detected with air shower experiments (Milagro, HAWC, Tibet AS and LHAASO), are from the tail. With this assumption, it is possible to explain the multi-wavelength spectrum of the head region with either a hadronic or leptonic model. Instead, the leptonic model fails to explain the $>$ 10 TeV and X-rays emission of the tail simultaneously, while the hadronic model can reproduce the observed spectrum at the tail with a cutoff power-law proton spectrum with a cutoff energy at $\sim$ 1 PeV.

The reults of our work have been extensively discussed in the recent publication [1], to which we refer readers for further details.

7th Heidelberg International Symposium on High-Energy Gamma-Ray Astronomy (Gamma2022)
4-8 July 2022
Barcelona, Spain

*Speaker

PoS(Gamma2022)029

1. Introduction

Recent progress in the air shower arrays such as HAWC, Tibet, and LHAASO enlarged the list of PeVatron candidates substantially. One of the most promising candidates is SNR G106.3+2.7. In the radio continuum, this SNRs shows a cometary shape with a bright and circular head and a tail extending towards south west (see Fig. 1). At the corner of the head, there is a pulsar wind nebula (PWN), encompassing an energetic pulsar, PSR J2227+6114. The Milagro, HAWC, Tibet ASγ, and LHAASO collaborations also reported on the detection of VHE γ-ray emission above tens of TeV from this source [e.g, 2, 3], which made it an intriguing object to study in the context of PeV cosmic ray accelerators. It was recently studied intensively also in X-rays [e.g., 4] and GeV gamma-rays [e.g, 5, 6]. VERITAS also reported a detection of extended very-high-energy (VHE) γ-ray emission above 630 GeV from the *tail* region, which was dubbed VER J2227+60[7]. We study this complex region using deep observations with the MAGIC telescopes, which provide a better angular resolution than the ones of previous γ-ray observations of G106.3+2.7.

2. Observations

The MAGIC telescopes are two 17 m diameter imaging Cherenkov telescopes located at 2200 m altitude above sea level at the Observatorio del Roque de los Muchachos on the Canary island La Palma, Spain (28.76° N; 17.89° W). At medium (30°–45°) zenith angles, the sensitivity of MAGIC varies such that a source as dim as 0.75% of the Crab Nebula can be detected with 5σ significance in 50 hours of observations, when integrating over energies above 200 GeV.

VER J2227+608 was observed from May 2017 to August 2019 at zenith angles between 30° and 50°, yeilding 122 hours of good quality data. The MAGIC angular resolution for this analysis using the so-called DISP method [8] was remarkable and found to be 0.084° (68% containment radius) at $E > 0.2$ TeV and 0.072° at $E > 1$ TeV. This is the best angular resolution among the previous γ-ray observations for this object.

3. Results

The emission maps around VER J2227+608/SNR G106.3+2.7 above 0.2 TeV are shown in the panel a) of Fig. 1. The morphology of the detected γ-ray emission clearly changes with energy, as can be seen in the panels b), c) and d) of Fig. 1. To better understand the emission mechanism, we defined two circular regions, centered at the *head* and the *tail* , (see Fig. 1 (a)) and analyzed them independently. The positions of them, (RA, DEC) = (337.°13, 61.°10) and (336.°72, 60.°84), were determined with a fit to the γ-ray map above 0.2 TeV with a double symmetric Gaussian, and their extension has been set by the maximum non-overlapping radius of 0.°16. The excesses are detected from the head and tail regions above 0.2 TeV with significances of 6.2σ and 6.9σ, respectively.

Fig. 2 presents the γ-ray spectra of the two regions and the extraction region of VER J2227+608 [7]. The spectra are fitted with a power-law function: $\frac{dN}{dE} = N_0 \left(\frac{E}{3\ \mathrm{TeV}}\right)^{-\Gamma}$ and the best-fit parameters are summarised in Table 1. For the VER J2227+608 region, the spectrum obatined with MAGIC is consistent with the one from VERITAS [7]. On the other hand, the γ-ray spectrum in the tail region has a higher flux and a marginally harder index than that of the head region.

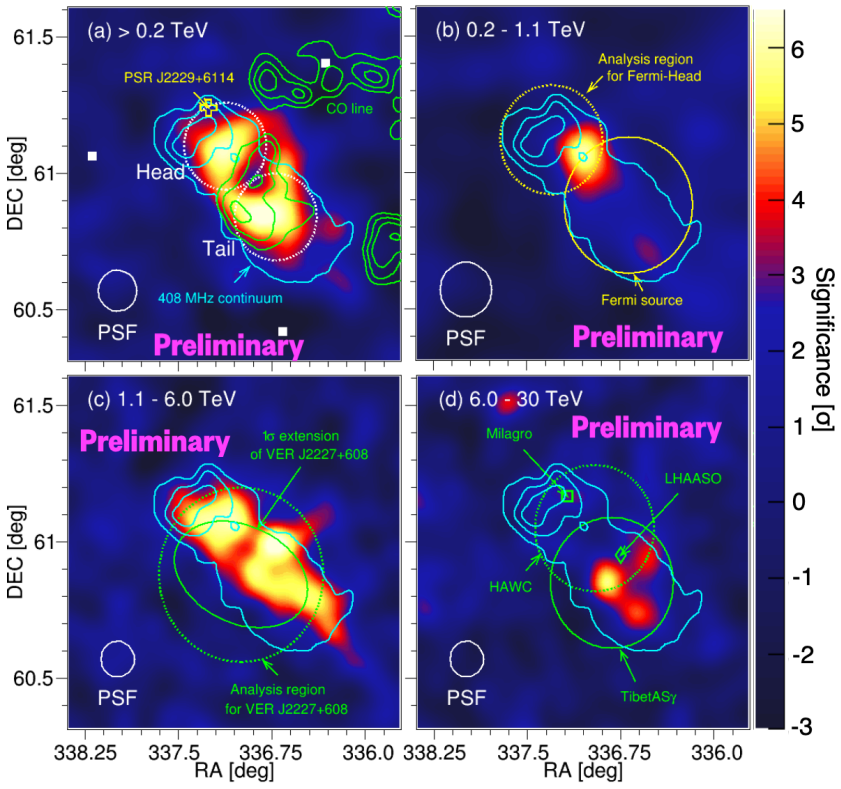

Figure 1: Energy-dependent significance maps of SNR G106.3+2.7 observed with the MAGIC telescopes. **(a)** Map above 0.2 TeV. The position of PSR J2229.0+6114 is marked with the open yellow cross. The cyan contours (overlaid on all panels) show the radio emission of SNR G106.3+2.7 at 408 MHz by DRAO [9]. The green contours represent the ^{12}CO ($J = 1-0$) line intensity. White squares denote the pointing positions used in the observations. **(b)** Map at 0.2–1.1 TeV. **(c)** Map at 1.1–6.0 TeV. The yellow ellipse and dotted circles represent the extended TeV γ-ray emission of VER J2227+608 and θ^2 cut region used in the VERITAS paper [7], respectively. **(d)** Map at 6.0–30 TeV. The open square and diamond show the centroid of the VHE γ-ray emission detected with Milagro [2] and LHAASO [3], respectively. The same picture can be found in [1]

Table 1: Best fit spectral parameters

Source	N_0 (10^{-14} cm^{-2} s^{-1} TeV^{-1}) at 3 TeV	Γ	χ^2/ndf
head	$3.8 \pm 0.7_{\rm stat} \pm 0.7_{\rm sys}$	$2.12 \pm 0.12_{\rm stat} \pm 0.15_{\rm sys}$	5.5/6
tail	$6.0 \pm 0.7_{\rm stat} \pm 1.0_{\rm sys}$	$1.83 \pm 0.10_{\rm stat} \pm 0.15_{\rm sys}$	2.6/6
VER J2227 (MAGIC)	$13.1 \pm 1.1_{\rm stat} \pm 2.1_{\rm sys}$	$1.91 \pm 0.07_{\rm stat} \pm 0.15_{\rm sys}$	7.1/6
VER J2227 [VERITAS, 7]	$11.5 \pm 2.7_{\rm stat} \pm 3.5_{\rm sys}$	$2.3 \pm 0.33_{\rm stat} \pm 0.30_{\rm sys}$	-

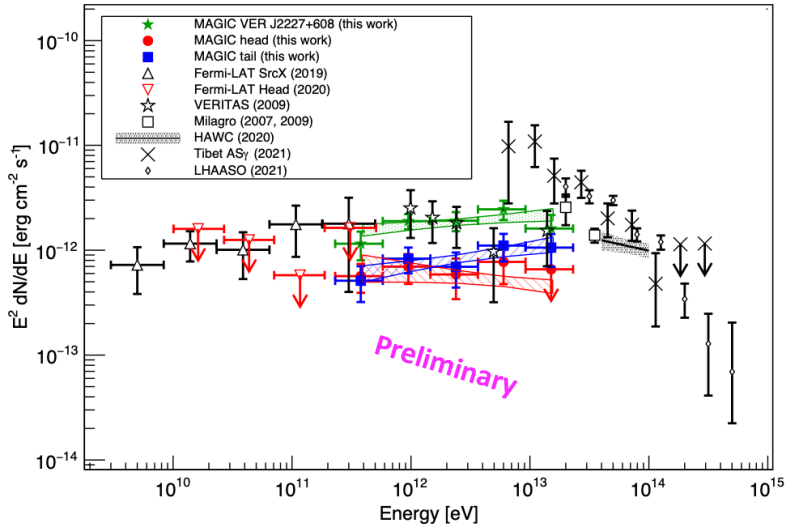

Figure 2: Spectral energy distribution of the whole region of SNR G106.3+2.7. Green data represent the spectrum of the VER J2227+608 region as measured with the MAGIC telescopes. Blue and red points are for the head and the tail region, respectively. The open triangles, open stars, open squares, x marks, and open diamonds show the *Fermi*-LAT [5], VERITAS [7], Milagro [2, 10], Tibet ASγ [11], and LHAASO measurements [3], respectively. The black bow-tie area shows a power-law fit and 1σ statistical errors measured by HAWC [12].

.

Table 2: Model parameters for reproducing the observed spectra. α and E_c are the power-law index and the cutoff energy of the particle spectrum, respectively. W is the total energy of particles with energy above 1 GeV. The subscript e and p denote electrons and protons. N_{gas} is the target gas density.

Model	Region	α_e α_e	$E_{c,e}$ [TeV]	W_e [erg]	B [μG]	α_p	$E_{c,p}$ [TeV]	W_p [erg]	N_{gas} [cm^{-3}]	χ^2/ndf
Leptonic	*head*	2.6	360	1.4×10^{47}	3	-	-	-	-	5.0/7
	tail	2.6	120	1.6×10^{47}	3	-	-	-	-	103.1/31
Hadronic	*head*	2.5	60	1.8×10^{46}	10	1.7	60	8.9×10^{45}	100	5.3/7
	tail	2.5	35	2.0×10^{46}	10	1.7	1000	8.2×10^{45}	200	39.9/31

4. Modelling and discussion

As shown in Fig. 1(d), the significant γ-ray emission above 6.0 TeV is detected in the *tail* region but not in the *head* region. In the following modeling and discussion, we assume that the measured emission above 10 TeV [e.g 2, 3] is only from the *tail* region. We also assume several parameters of its environment. The details of the modelling (including how to treat observational results in 10 – 100 TeV region) and more physics discussion can be found in the recent publication [1]

4.1 *Head* region

Our modeling shows that X-ray and gamma-ray fluxes can be explained with leptonic emission from the same electron population. Using the electron cutoff energy ($E_{c,e}$) and the magnetic-field

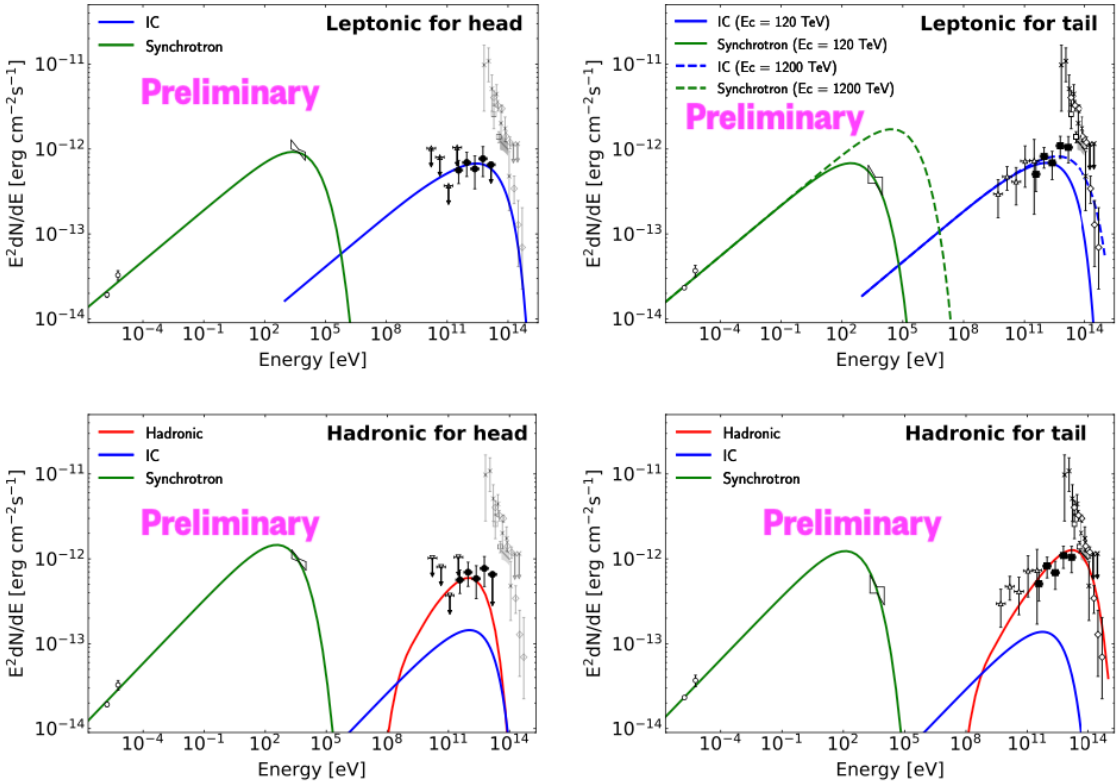

Figure 3: Modeling of the SED of SNR G106.3+2.7. The left and right panels show the results of the head and the tail, respectively. The upper and lower panels show the results of the leptonic and hadronic models, respectively. The white circles show the radio flux of each region [9]. The black bow-tie area shows a power-law fit and 1σ statistical errors measured by Suzaku [4]. The open triangles show the *Fermi*-LAT measurements [5, 6]. The markers in the TeV γ-ray band are the same as in Fig. 2. In the top-right panel, the solid and dashed lines show the leptonic emission with the energy cutoff of 120 and 1200 TeV, respectively.

strength (B) estimates from the leptonic model, we calculate the electron lifetime due to synchrotron losses to be ~3.9 kyr $(E_{c,e}/360\ \mathrm{TeV})^{-1}(\mathrm{B}/3\ \mu\mathrm{G})^{-2}$. This is consistent with the age of the SNR estimated to be 3.9 kyr from the spectral break in the radio spectrum of the PWN [13]. Hadronic scenario also works for the head. The protons accelerated up to 60 TeV can explain the VHE γ-ray emission detected by MAGIC, given the presence of dense HI clouds in the *head* region. Still electrons with a largely different spectral index are needed to explain the radio and X-ray emission.

4.2 *Tail* region

It is difficult to explain the *tail* emission with the leptonic model. The γ-ray spectrum of the *tail* region can be reproduced with the hadronic model, assuming a proton maximum energy of 1 PeV (χ^2/ndf = 39.9/31). Generally speaking, acceleration up to 1 PeV can only be achieved at the early stages (< 1.0 kyr) of the SNR evolution [e.g., 14]. This contradiction in the SNR age can be solved assuming a CR-escape scenario [e.g. 15]. In this scenario, protons accelerated up to ~ PeV energies at a young SNR escape from acceleration regions and illuminate nearby clouds, which produce "delayed" γ-ray emission.

5. Summary

The MAGIC observations of SNR G106.3+2.7 achieved a significant detection of TeV γ rays from the *head* and the *tail* regions separately for the first time. Under the assumption that the γ-ray emission above 10 TeV is only from the *tail* region, the *head* emission can be explained with both a hadronic and a leptonic model, while the leptonic model of the *tail* region is in contradiction with the X-ray flux. A proton spectrum with a cutoff at $\sim$ 1 PeV could explain the observed spectrum from the *tail* region. This suggests that protons accelerated in the SNR shock in the past escaped from the SNR and interacted with target gas located in front of the SNR along the line of sight. This scenario could also explain the inconsistency between the SNR age and maximum energy of accelerated protons.

Acknowledgments

We acknowledge the support from the agencies and organizations listed here: https://magic.mpp.mpg.de/ack_public_2022_05/

References

[1] MAGIC Collaboration et al. *A&A*, 671:A12, 2023.

[2] A. A. Abdo et al. *Astrophys. J.*, 700:L127–L131, 2009.

[3] C. Zhen et.al. *Nature*, 594(7861):33–36, 2021.

[4] Y. Fujita et al. *The Astrophysical Journal*, 912(2):133, may 2021.

[5] Y. Xin et al. *The Astrophysical Journal*, 885(2):162, nov 2019.

[6] Siming Liu, Houdun Zeng, Yuliang Xin, and Hui Zhu. *Astrophys. J.*, 897(2):L34, 2020.

[7] V. A. Acciari et al. *Astrophys. J.*, 703:L6–L9, 2009.

[8] J. Aleksić et al. *Astroparticle Physics*, 35(7):435–448, 2012.

[9] Serge Pineault and Gilles Joncas. *The Astronomical Journal*, 120(6):3218–3225, dec 2000.

[10] A.A. Abdo et al. *Astrophys. J.*, 664:L91–L94, 2007.

[11] M. Amenomori et al. *Nature Astron.*, 5(5):460–464, 2021.

[12] A. Albert et al. *Astrophys. J. Lett.*, 896:L29, 2020.

[13] Roland Kothes, Wolfgang Reich, and Bülent Uyanıker. 638(1):225–233, Feb 2006.

[14] AR Bell, KM Schure, B Reville, and G Giacinti. *Mon. Not. Roy. Astron. Soc.*, 431:415, 2013.

[15] Stefano Gabici and Felix A. Aharonian. *Astrophys. J. Lett.*, 665:L131, 2007.